ACS Photonics

Letter

pubs.acs.org/journal/apchd5

Enhanced Magnetic Second-Harmonic Generation from Resonant Metasurfaces

Sergey Kruk,*[,†] Martin Weismann,[‡,§] Anton Yu. Bykov,[⊥] Evgeniy A. Mamonov,[⊥] Irina A. Kolmychek,[⊥] Tatiana Murzina,[⊥] Nicolae C. Panoiu,[‡] Dragomir N. Neshev,[†] and Yuri S. Kivshar[†]

[†]Nonlinear Physics Centre and Centre for Ultrahigh Bandwidth Devices for Optical Systems (CUDOS), Australian National University, Canberra, ACT 0200, Australia

[‡]Department of Electronic and Electrical Engineering, University College London, London WC1E 7JE, U.K.

[§]Photon Design Ltd, 34 Leopold Street, Oxford OX4 1TW, U.K.

[⊥]Physics Department, Lomonosov Moscow State University, Moscow 119991, Russia

Supporting Information

ABSTRACT: We study, both experimentally and theoretically, the second-order nonlinear response from resonant metasurfaces composed of metal−dielectric nanodisks. We demonstrate that by exciting the resonant optical modes of the composite nanoparticles we can achieve strong enhancement of the second-harmonic signal from the metasurface. By employing a multipole expansion method for the generated second-harmonic radiation, we show that the observed SHG enhancement is due to the magnetic dipolar and electric quadrupolar second-order nonlinear response of the metasurface.

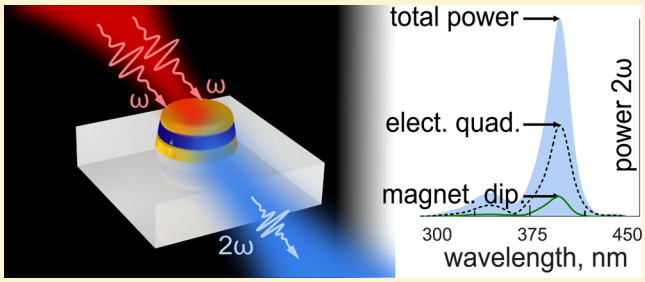

KEYWORDS: *nonlinear optics, second-harmonic generation, plasmonic nanoparticles, optical magnetism, multipole decomposition*

The nonlinear optical properties of nanostructures are known to differ substantially from those of bulk media because they are affected by strong confinement and local resonances.[1−7] It is well established that the strong field enhancement through formation of "hot spots" can dramatically boost nonlinear effects in metallic nanoparticles.[8−11] Importantly, in the case of metamaterials, the nanopatterning leads not only to more efficient nonlinear interaction but also to completely new nonlinear regimes due to the magnetic optical response of the constituent "meta-atoms". While exciting applications of the linear magnetic response of metamaterials for both metallic[12−16] and dielectric[17−19] structures have been readily achieved at infrared and even optical frequencies, the magnetic nature of nonlinear optical phenomena in metamaterials is still largely unexplored.

We focus our attention on the process of second-harmonic generation (SHG), which is an even-order nonlinear process that vanishes in centrosymmetric materials in the electric dipole approximation.[20] For small nanoparticles, efficient SHG may be observed due to several factors, including local field enhancement, deviation of the particle shapes from a symmetric one, and surface effects.[21] Importantly, the resonances in plasmonic and dielectric nanoparticles, combined with a strong enhancement of the optical near-field, as well as the effective overlap of the interacting optical modes, allow for multifold enhancement of SHG.[22−24]

The enhancement of efficiency of second-harmonic generation within extremely small nanoscopic volumes is of paramount interest in surface science,[25,26] colloidal chemistry,[27] and catalytic chemistry.[28] Due to its nature, second-harmonic generation is extremely sensitive to surface adsorbents. As such, even a single-molecule layer adsorbed onto a surface can completely change the surface nonlinear susceptibility. This sensitivity to changes of the chemical environment has found many applications to the study of the symmetry properties of surfaces, the nature of adsorbates at surfaces or interfaces, or noninvasive probing of buried interfaces.

It was recognized that the local field distribution depends drastically on the size, shape, and mutual orientation of the nanoparticles, thus providing a way for the design of artificial materials with required nonlinear optical properties.[29−31] Such nonlinearity engineering resembles the engineering of nonlinear materials by chemical composition, where molecules of different symmetries can be selected to enable the required nonlinear polarization.[32,33] However, the top-down approach enables the ultimate design of any arbitrary nonlinear polarization.

Most of the research in this field was performed for various types of (asymmetric) plasmonic nanoparticles where the field localization effects are much more pronounced. Plasmonic

Received: April 27, 2015
Published: July 27, 2015

DOI: 10.1021/acsphotonics.5b00215
ACS Photonics 2015, 2, 1007−1012

metasurfaces exhibiting both electric and magnetic resonances have also been studied, aiming at obtaining magnetic nonlinear response from such metasurfaces. In particular, works on SHG in split-ring resonator metasurfaces[31,34,35] have described the SHG signal as a contribution from the Lorentz force exerted on the electrons oscillating in the split rings. However, the exact contribution of the magnetic nonlinearity was not quantified. Other works on fishnet metal−dielectric−metal metasurfaces have attributed the SHG signal predominantly to the surface SHG contribution, without the presence of magnetic nonlinearity.[36] These discrepancies have created a certain controversy about the nature of the observed harmonic generation from such resonant metasurfaces, namely, if it arises from the electric or magnetic nonlinear polarization of the metasurfaces. Subsequent works have provided a theoretical description of the physical mechanisms for achieving magnetic and electric nonlinear responses;[37,38] however experimental verification in optics is still missing. In particular, the possibility to engineer the electric and magnetic nonlinear polarizabilities of the metasurface and the subsequent interference of second-harmonic waves can have important implications for directional nonlinear generation as proposed earlier.[39] Therefore, further studies about the exact origin, electric or magnetic, of the process of SHG from resonant metasurfaces are required.

In this Letter, we analyze experimentally and theoretically the SHG from an optical metasurface of metal−dielectric−metal nanodisks in the vicinity of optically induced electric and magnetic resonances. We demonstrate that resonant excitation of different modes of nanoparticles allows for strong enhancement of the SHG signal near the optically induced magnetic resonance. The related theoretical analysis further shows that the SHG intensity is a result of the electric quadrupolar and magnetic dipolar contributions of the nonlinear material polarization.

EXPERIMENTAL RESULTS

For our experiments, we employ metasurfaces formed by a regular array of metal−dielectric−metal disk-like nanoparticles (meta-atoms). We use two metal disks separated by a dielectric layer to obtain two distinct resonant modes of the meta-atom excited by incident light at two different wavelengths.[40,41] The two resonances are associated with co- and counter-propagating electric currents excited in the parallel metal disks. In particular, the counter-propagating electric currents result in nonzero electric quadrupole and magnetic dipole linear response in the meta-atoms and are therefore referred to below as magnetic resonances of the metasurface.

The SEM image of the fabricated metasurface is shown in Figure 1a. The inset shows a side view of a single meta-atom (see Supporting Information for details on the fabrication procedure and sample dimensions).

We study the second-order optical response of the metasurface for both TM and TE polarizations of the pump beam and different angles of incidence φ, as shown schematically in Figure 1b,c. The sample is illuminated from the top side (fundamental beam spot size of ∼50 μm), and the TM-polarized second-harmonic signal is collected from the substrate side.

First, we measure the linear transmission of the metasurface at normal incidence, as shown in Figure 2a, gray curve.

The spectra feature two resonances centered at 640 and 790 nm wavelengths. The SHG spectroscopy is studied experimentally by employing a titanium−sapphire laser (100 fs

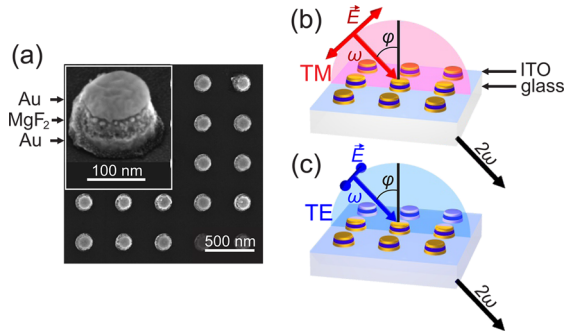

Figure 1. (a) SEM image of a fabricated metasurface. Inset shows a side view of a single three-layer meta-atom made of Au/MgF_2/Au layers. (b, c) Geometry of the SHG experiment for TM- and TE-polarized pump waves, respectively.

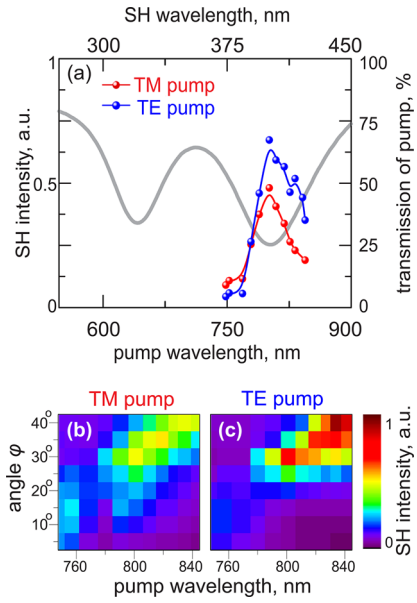

Figure 2. Experimental results. (a) Linear transmission of the metasurface (gray) at normal incidence and second-harmonic spectra for TM- and TE-polarized pump waves (red and blue) measured for the incident angle of 30°. (b, c) Second-harmonic intensity vs pump wavelength and angle of incidence for TM and TE polarizations.

pulses, 80 MHz repetition rate, tuning range from 720 to 855 nm, peak intensity in the focal plane ∼0.3 GW/cm^2) as a source of the fundamental radiation. The SHG radiation transmitted through the sample is collected by a lens with 0.17 NA and is spectrally selected by a set of color filters and a monochromator. Design parameters of the metasurface are chosen in such a way that the second long-wavelength resonance falls within the tunability range of the laser. The SHG signal is detected by spectral measurements and exhibits a square-law dependence on the pump intensity. In addition, we verify that the spectra of the nonlinear signal correspond to the spectrum of second harmonic (see details in the Supporting Information).

Figure 2a shows the spectra of the SH intensity measured at the incidence angle $\varphi = 30°$ for two linear polarizations of the fundamental laser beam (red and blue, respectively). Both SH spectra show a pronounced efficiency enhancement near the resonance at 790 nm wavelength. Figure 2b,c show the angular dependence of the SH spectra for the two polarizations. We note that at normal incidence the SHG efficiency nearly

DOI: 10.1021/acsphotonics.5b00215
ACS Photonics 2015, 2, 1007−1012

vanishes, and the SHG from the substrate remains below the noise level for all angles of incidence. The vanishing SHG at normal incidence is expected because the design of the metasurface elements is close to centrosymmetric, even with the presence of a substrate and a tilting shape of the meta-atoms, and hence the SHG process is almost prohibited. In contrast, for oblique incidence surface dipoles contribute effectively into the frequency conversion, and the SHG process becomes more efficient with an increase of the incident angle φ. In addition, we observe a red-shift of the SH spectral maxima with an increase of the incidence angle φ for both TE and TM polarizations of the fundamental beam.

THEORETICAL INSIGHTS

In order to gain a deeper insight into our experimental results and the physical nature of the SHG process in resonant metasurfaces, we perform numerical calculations of the SH spectrum and analyze its origin as a result of the emission of electric and magnetic multipoles. We first calculate the linear transmission for normal incidence (shown in Figure 3a, gray

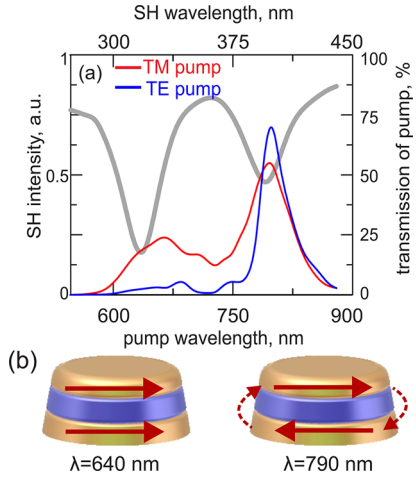

Figure 3. (a) Numerical transmission spectrum of the metasurface at normal incidence (gray) and SH spectra for TM- and TE-polarized pumps (red and blue, respectively) calculated for the incidence angle ϕ = 30°. (b) Schematic of the electric currents distribution in a single meta-atom at the first and second resonant wavelengths. Dashed lines visualize the displacement current.

curve) and for 30° oblique incidence (shown in Supporting Information). The linear spectra are determined by using the generalized-source method (GSM).[42] To validate these results, the transmission spectra are also calculated by using CST Microwave Studio. The positions of the resonances in the calculated spectra are in a good agreement with the experimental data, corresponding to an electric resonance at approximately 640 nm and a magnetic one at 790 nm. The transmission spectra at normal incidence are qualitatively similar to the spectra at oblique incidence. A small red-shift of the resonant wavelength can be observed for the oblique excitation. At the first resonance near 640 nm, copropagating currents are excited in the top and bottom metallic nanodisks of the meta-atom. At the second resonance, counter-propagating currents are excited in the two metallic nanodisks (see Figure 3b). However, the physical nature of these resonances is best revealed by applying the multipolar expansion method for the sources of the scattered field, namely, the electric charges and currents of the meta-atom, in accord with the definitions

$$\mathbf{p}_\omega = \int \mathbf{P}_\omega(\mathbf{r})\, d\mathbf{r} \tag{1a}$$

$$\mathbf{m}_\omega = -i\frac{\omega}{2}\int \mathbf{r}\times\mathbf{P}_\omega(\mathbf{r})\, d\mathbf{r} \tag{1b}$$

$$Q_{\omega,jk} = \int [3(r_j P_{\omega,k} + r_k P_{\omega,j}) - 2\delta_{jk}\mathbf{r}\cdot\mathbf{P}_\omega(\mathbf{r})]\, d\mathbf{r} \tag{1c}$$

Here $\mathbf{P}_\omega(\mathbf{r}) = \varepsilon_0[\varepsilon_r(\omega) - 1]\mathbf{E}_\omega(\mathbf{r})$ is the polarization at the location point $\mathbf{r}$, with $\mathbf{E}_\omega(\mathbf{r})$ being the electric field and ε_r the relative electric permittivity, and $\mathbf{p}_\omega$, $\mathbf{m}_\omega$, and $Q_{\omega,jk}$ are the electric dipole, magnetic dipole, and electric quadrupole of the nanodisk meta-atom, respectively. Importantly, eqs 1 include the contributions of both displacement and conductive currents if the frequency dispersion of ε_r is taken into account. We notice that, since the contribution of the substrate into the far-field is shown to be negligible within the experimental accuracy, the integration in eqs 1 is restricted to the volume of the meta-atom.

We perform the multipolar expansion using eqs 1 that provides us with a quantitative analysis of the sources of the far field at the pump. The results of this analysis are summarized in Figure 4a,b, and they suggest that the first resonance originates

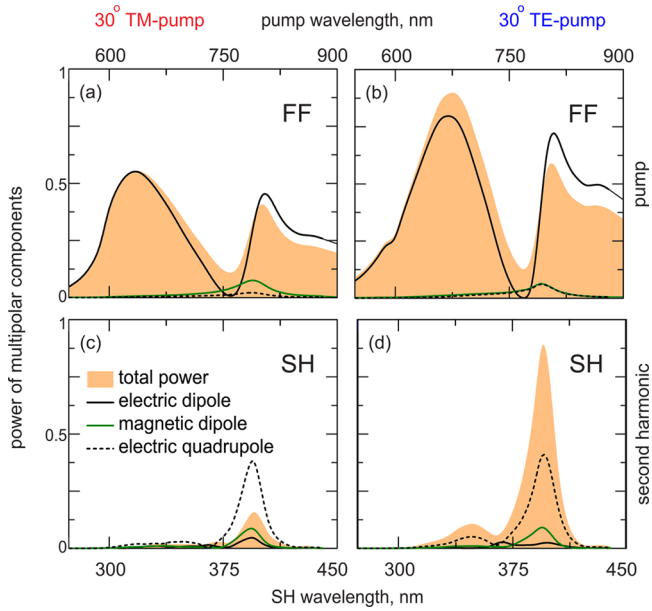

Figure 4. Numerically calculated cross sections of the electric dipole (black, solid), electric quadrupole (black, dashed), and magnetic dipole (green) at (a, b) fundamental wavelengths and (c, d) second-harmonic wavelengths, for two polarizations of the pump at the oblique incidence.

from the excitation of an electric dipole, whereas the second spectral peak corresponds to the excitation of a mixture of magnetic dipole and electric quadrupole moments resonantly excited together with the electric dipole. In addition, it can be seen that, for both types of pump polarization, for wavelengths smaller than the wavelength of the magnetic resonance, the radiation emitted by the multipoles interferes constructively so that the total radiated power is higher than the power produced solely by the electric dipole. In the spectral region of the magnetic resonance and beyond, destructive interference is

DOI: 10.1021/acsphotonics.5b00215
ACS Photonics 2015, 2, 1007−1012

observed and the total radiated power becomes lower than that of the electric dipole alone.

The nonlinear optical response of the array of meta-atoms at the SH comprises several possible contributions, namely, the surface (local) and bulk (nonlocal) SHG from the metallic nanodisks, as well as bulk (local) SHG from metallic disks and the MgF_2 dielectric layer. However, because of the centrosymmetric nature of the Au crystalline lattice and polycrystalline structure of MgF_2, the last two contributions can be neglected. As a result, the sources of the SH field can be described by the following nonlinear polarizations:[43]

$$\mathbf{P}^{s}_{\Omega}(\mathbf{r}) = \epsilon_0 \hat{\chi}^{(2)}_s : \mathbf{E}_{\omega}(\mathbf{r})\, \mathbf{E}_{\omega}(\mathbf{r})\, \delta(\mathbf{r} - \mathbf{r}_s) \tag{2a}$$

$$\mathbf{P}^{b}_{\Omega}(\mathbf{r}) = \delta'(\mathbf{E}_{\omega}(\mathbf{r})\cdot\nabla)\mathbf{E}_{\omega}(\mathbf{r}) + \beta\mathbf{E}_{\omega}(\mathbf{r})(\nabla\cdot\mathbf{E}_{\omega}(\mathbf{r})) + \gamma\nabla(\mathbf{E}_{\omega}(\mathbf{r})\cdot\mathbf{E}_{\omega}(\mathbf{r})) \tag{2b}$$

where $\mathbf{P}^{s}_{\Omega}$ and $\mathbf{P}^{b}_{\Omega}$ describe the surface and bulk nonlinear polarization, respectively, and $\mathbf{r}_s$ defines the surface. The surface of metallic parts of the meta-atom possesses an isotropic mirror-symmetry plane perpendicular to the surface, so that the surface second-order susceptibility tensor, $\hat{\chi}^{(2)}_s$, has only three independent components, $\hat{\chi}^{(2)}_{s,\perp\perp\perp}$, $\hat{\chi}^{(2)}_{s,\perp\parallel\parallel}$, and $\hat{\chi}^{(2)}_{s,\parallel\parallel\perp} = \hat{\chi}^{(2)}_{s,\parallel\perp\parallel}$, where the symbols $\perp$ (or $\parallel$) refer to the directions normal (or tangent) to the surface. For gold, the corresponding values are[44] $\hat{\chi}^{(2)}_{s,\perp\perp\perp} = -(0.86 + 1.34\mathrm{i}) \times 10^{-18}$ m^2 V^{-1} and $\hat{\chi}^{(2)}_{s,\parallel\parallel\perp} = -(4.61 + 0.43\mathrm{i}) \times 10^{-20}$ m^2 V^{-1}. $\hat{\chi}^{(2)}_{s,\perp\parallel\parallel}$ can be neglected as compared with other components, whereas the bulk susceptibility is $\gamma = 7.13 \times 10^{-21}$ m^2 V^{-1}. Moreover, the dominant contribution to the bulk polarization comes from the third term in eq 2b, as in homogeneous media the second term vanishes and the ratio between the first and third terms is about ν/ω, where ν is the damping frequency (at optical frequencies, $\nu \ll \omega$);[45] therefore, in our simulations we set $\delta' = \beta = 0$. Note that we did not include in eq 2b a fourth term that accounts for the anisotropy of the medium because in our system the nonlinear bulk polarization is due entirely to the free electrons; namely, it is generated in an isotropic medium.

To calculate the response at the SH frequency, we use a recently developed nonlinear extension to GSM.[46] This nonlinear GSM is an efficient frequency domain method for solving the problems of light diffraction by periodic structures containing both linear and nonlinear optical media. It consists of three steps: (i) Determine the electromagnetic field at the FF pump wavelength using the linear GSM; (ii) calculate nonlinear SH polarizations using eqs 2; and (iii) add this polarization to the linear polarization and use again the linear GSM to compute the electromagnetic fields at the SH frequency as well as the corresponding transmission and reflection coefficients. The SH spectra for two linear polarizations of a pump determined by this approach are shown in Figure 3a. Both SHG theoretical spectra are in a good agreement with the experimental data, and they show pronounced maxima near the second (magnetic) resonance at around 790 nm. Importantly, the theory predicts less efficient SHG near the first (electric) resonance at 640 nm.

The red-shift of the SH resonance appears in the metasurface because its constituent meta-atoms act as an array of driven coupled harmonic oscillators. Thus, when the angle of incidence increases, the incoming field couples more efficiently to and excites the resonances of the meta-atom. As a result, the optical near field of the resonators becomes more localized, and therefore the overlap between the optical modes of the meta-atoms in the array decreases. In our coupled oscillators model this translates to a reduced coupling constant and, consequently, a reduced resonance frequency.

To understand the difference in the SHG efficiency observed at the two resonances, we employ a multipole expansion of the sources of the nonlinear field using a similar approach to that used at the FF. Specifically, we calculate numerically the distributions of nonlinear electric currents and charges induced in the meta-atoms by the optical pump and, subsequently, by using eqs 1 and 2, the nonlinear multipoles $\mathbf{p}_{\Omega}$, $\mathbf{m}_{\Omega}$, and $Q_{\Omega,ij}$ associated with these distributions.[47,48] We emphasize that in these calculations we consider only the nonlinear source polarizations given in eqs 2, with the linear polarization of the medium at the SH frequency being excluded. Consequently, the resonant effects due to geometrical and material characteristics of the meta-atom on the radiative properties of these multipoles are not incorporated into our analysis, which implies that the multipoles are assumed to radiate as if they were in a vacuum. By doing this, we want to separate the purely nonlinear properties of those multipoles from the linear properties in the spectral region of the second-harmonic generation. We follow this procedure to calculate the spectra of the first three terms of the multipolar expansion, namely, the electric dipole, magnetic dipole, and electric quadrupole, induced in the meta-atom by a pump wave incident onto the metasurface at the angle $\varphi = 30°$.

Starting from the nonlinear optical response of a single meta-atom, we can now proceed to study the nonlinear properties of a metasurface created by a periodic square lattice of such meta-atoms as described by eq I.11 of the Supporting Information. The power spectra corresponding to the three types of multipoles, as well as the spectrum of the total emitted power, are presented in Figure 4c and d for both TM- and TE-polarized pump, respectively. While there are quantitative differences between these SHG spectra and those obtained using rigorous calculations based on the GSM (see Figure 3a), both methods predict the same qualitative features of the SHG spectra, namely, two spectral peaks corresponding to the electric and magnetic resonances, which are separated by a spectral region of weak SHG. More specifically, the radiated SHG intensity is dominated by the higher-order multipoles, electric quadrupole, and magnetic dipole, with less than 3% contribution from the electric dipole.

Note that the spectral location of this weak SHG region, which can also be observed in the experimentally measured spectra (see Figure 2b and c), is essentially independent of the angle of incidence of the FF beam. This observation confirms our theoretical predictions of a vanishing nonlinear dipole moment at this particular frequency. In addition, similarly to the linear optical response of the metasurface, these spectra illustrate that the nonlinear properties of the metasurface are determined by subtle interference effects among the radiation emitted by the three different types of multipoles, as observed in Figure 4c,d.

CONCLUSIONS

We have studied the second-harmonic generation from metasurfaces composed of metal−dielectric−metal nanodisks, which are known to support both electric and magnetic dipole resonances. We have experimentally observed that the intensity of the second-harmonic signal exhibits strong enhancement

DOI: 10.1021/acsphotonics.5b00215
ACS Photonics 2015, 2, 1007−1012

near the magnetic resonance of the metasurface, which agrees well with numerical calculations. We have shown that this strong enhancement of the second-harmonic intensity is a superposition of magnetic dipole and electric quadrupole modes induced by the pump wave at oblique incidence. We believe these results will pave the way to establishing novel engineered nonlinear materials with enhanced harmonic efficiency, driven by optically induced magnetic resonances. This will find immediate applications in colloidal chemistry, surface science, and catalytic chemistry.[25−28]

■ ASSOCIATED CONTENT

Supporting Information

The Supporting Information is available free of charge on the ACS Publications website at DOI: 10.1021/acsphotonics.5b00215.

Details on theoretical derivations of the equation for the light intensity emitted by a metasurface, a wide range of linear and nonlinear spectra, details of nanofabrication, and estimations of nonlinear conversion efficiencies (PDF)

■ AUTHOR INFORMATION

Corresponding Author

*E-mail: Sergey.Kruk@anu.edu.au.

Notes

The authors declare no competing financial interest.

■ ACKNOWLEDGMENTS

The authors acknowledge useful comments from M. Kauranen and A. Zayats, as well as support from the Australian Research Council, the Russian Foundation for Basic Research (grant 14-02-00446), the Royal Society's International Exchanges Scheme, and a UCL Impact Award graduate studentship funded by UCL and Photon Design Ltd.

■ REFERENCES

(1) Kreibig, U.; Vollmer, M. *Optical Properties of Metal Clusters*; Springer-Verlag: Berlin, 1995.

(2) Barnes, W. L.; Dereux, A.; Ebbesen, T. W. *Nature* **2003**, *424*, 824.

(3) Zayats, A. V.; Smolyaninov, I. I.; Maradudin, A. A. *Phys. Rep.* **2005**, *408*, 131.

(4) Maier, S. A. *Plasmonics: Fundamentals and Applications*; Springer: New York, 2007.

(5) Panoiu, N. C.; Osgood, R. M. Subwavelength nonlinear plasmonic nanowire. *Nano Lett.* **2004**, *4*, 2427−2430.

(6) Suh, J. Y.; Odom, T. W. Nonlinear properties of nanoscale antennas. *Nano Today* **2013**, *8*, 469−479.

(7) Shcherbakov, M. R.; Neshev, D. N.; Hopkins, B.; Shorokhov, A. S.; Staude, I.; Melik-Gaykazyan, E. V.; Decker, M.; Ezhov, A. A.; Miroshnichenko, A. E.; Brener, I.; Fedyanin, A. A.; Kivshar, Y. S. Enhanced Third-Harmonic Generation in Silicon Nanoparticles Driven by Magnetic Response. *Nano Lett.* **2014**, *14*, 6488−6492.

(8) van Nieuwstadt, J. A. H.; Sandtke, M.; Harmsen, R. H.; Segerink, F. B.; Prangsma, J. C.; Enoch, S.; Kuipers, L. Strong Modification of the Nonlinear Optical Response of Metallic Subwavelength Hole Arrays. *Phys. Rev. Lett.* **2006**, *97*, 146102.

(9) Fan, W.; Zhang, S.; Panoiu, N.-C.; Abdenour, A.; Krishna, S.; Osgood, R. M.; Malloy, K. J.; Brueck, S. R. J. Second harmonic generation from a nanopatterned isotropic nonlinear material. *Nano Lett.* **2006**, *6*, 1027.

(10) Kauranen, M.; Zayats, A. V. Nonlinear plasmonics. *Nat. Photonics* **2012**, *6*, 737−748.

(11) Celebrano, M.; Wu, X.; Baselli, M.; Großmann, S.; Biagioni, P.; Locatelli, A.; De Angelis, C.; Cerullo, G.; Osellame, R.; Hecht, B.; Duò, L.; Ciccacci, F.; Finazzi, M. Mode matching in multiresonant plasmonic nanoantennas for enhanced second harmonic generation. *Nat. Nanotechnol.* **2015**, *10*, 412−417.

(12) Pendry, J. B.; Holden, A. J.; Robbins, D. J.; Stewart, W. J. *IEEE Trans. Microwave Theory Tech.* **1999**, *47*, 2075.

(13) Linden, S.; Enkrich, C.; Wegener, M.; Zhou, J. F.; Koschny, T.; Soukoulis, C. M. Magnetic response of metamaterials at 100 terahertz. *Science* **2004**, *306*, 1351−1353.

(14) Yen, T. J.; Padilla, W. J.; Fang, N.; Vier, D. C.; Smith, D. R.; Pendry, J. B.; Basov, D. N.; Zhang, X. Terahertz magnetic response from artificial materials. *Science* **2004**, *303*, 1494−1496.

(15) Zhang, S.; Fan, W. J.; Minhas, B. K.; Frauenglass, A.; Malloy, K. J.; Brueck, S. R. J. Midinfrared resonant magnetic nanostructures exhibiting a negative permeability. *Phys. Rev. Lett.* **2005**, *94*, 037402.

(16) Butet, J.; Thyagarajan, K.; Martin, O. J. F. Ultrasensitive optical shape characterization of gold nanoantennas using second harmonic generation. *Nano Lett.* **2013**, *13*, 1787−1792.

(17) Etxarri, G. A.; Medina, G. R.; Perez, F. L. S.; Lopez, C.; Chantada, L.; Scheffold, F.; Aizpurua, J.; Vesperinas, N. M.; Saenz, J. J. Strong magnetic response of submicron Silicon particles in the infrared. *Opt. Express* **2011**, *19*, 4815−4826.

(18) Kuznetsov, A. I.; Miroshnichenko, A. E.; Fu, Y. H.; Zhang, J.; Lukyanchuk, B. Magnetic light. *Sci. Rep.* **2012**, *2*, 492.

(19) Liu, S.; Sinclair, M. B.; Mahony, T. S.; Jun, Y. C.; Campione, S.; Ginn, J.; Bender, D. A.; Wendt, J. R.; Ihlefeld, J. F.; Clem, P. G.; Wright, J. B.; Brener, I. Optical magnetic mirrors without metals. *Optica* **2014**, *1*, 250−256.

(20) Burns, W. K.; Bloembergen, N. Third-Harmonic Generation in Absorbing Media of Cubic or Isotropic Symmetry. *Phys. Rev. B* **1971**, *4*, 3437−3450.

(21) Aktsipetrov, O.; Elyutin, P.; Nikulin, A.; Ostrovskaya, E. Size effects in optical second-harmonic generation by metallic nanocrystals and semiconductor quantum dots: The role of quantum chaotic dynamics. *Phys. Rev. B: Condens. Matter Mater. Phys.* **1995**, *51*, 17591−17599.

(22) Lamprecht, B.; Leitner, A.; Aussenegg, F. SHG studies of plasmon dephasing in nanoparticles. *Appl. Phys. B: Lasers Opt.* **1999**, *68*, 419−423.

(23) Tuovinen, H.; Kauranen, M.; Jefimovs, K.; Vahimaa, P.; Vallius, T.; Turunen, J.; Tkachenko, N. V.; Lemmetyinen, H. linear and second-order nonlinear optical properties of arrays of noncentrosymmetric gold nanoparticles. *J. Nonlinear Opt. Phys. Mater.* **2002**, *11*, 421−432.

(24) Canfield, B. K.; Kujala, S.; Jefimovs, K.; Turunen, J.; Kauranen, M. Linear and nonlinear optical responses influenced by broken symmetry in an array of gold nanoparticles. *Opt. Express* **2004**, *12*, 5418−5423.

(25) Heinz, T. F. Second-order nonlinear optical effects at surfaces and interfaces. *Nonlinear Surf. Electromagn. Phenomena* **1991**, 353.

(26) Eisenthal, K. B. Liquid Interfaces Probed by Second-Harmonic and Sum-Frequency Spectroscopy. *Chem. Rev.* **1996**, *96*, 1343−1360.

(27) Eisenthal, K. B. Second Harmonic Spectroscopy of Aqueous Nano- and Microparticle Interfaces. *Chem. Rev.* **2006**, *106*, 1462−1477.

(28) Corn, R. M.; Higgins, D. A. Optical second harmonic generation as a probe of surface chemistry. *Chem. Rev.* **1994**, *94*, 107−125.

(29) Kujala, S.; Canfield, B.; Kauranen, M.; Svirko, Y.; Turunen, J. Multipole Interference in the Second-Harmonic Optical Radiation from Gold Nanoparticles. *Phys. Rev. Lett.* **2007**, *98*, 167403.

(30) Czaplicki, R.; Husu, H.; Siikanen, R.; Makitalo, J.; Kauranen, M.; Laukkanen, J.; Lehtolahti, J.; Kuittinen, M. Enhancement of Second-Harmonic Generation from Metal Nanoparticles by Passive Elements. *Phys. Rev. Lett.* **2013**, *110*, 093902.

(31) Valev, V. K.; et al. Second-Harmonic Generation from Magnetic Metamaterials. *Adv. Mater.* **2014**, *26*, 4074−4081.

(32) Zyss, J. *Molecular Nonlinear Optics: Materials, Physics, and Devices*; Academic Press: Boston, 1994; Vol. *260*.

DOI: 10.1021/acsphotonics.5b00215
ACS Photonics 2015, 2, 1007−1012

(33) Sioncke, S.; Verbiest, T.; Persoons, A. Second-order nonlinear optical properties of chiral materials. *Mater. Sci. Eng., R* **2003**, *42*, 115−155.
(34) Klein, M. W.; Enkrich, C.; Wegener, M.; Linden, S. Second-Harmonic Generation from Magnetic Metamaterials. *Science* **2006**, *313*, 502−504.
(35) Klein, M. W.; Wegener, M.; Feth, N.; Linden, S. Experiments on second- and third-harmonic generation from magnetic metamaterials. *Opt. Express* **2007**, *15*, 5238−5247.
(36) Kim, E.; Wang, F.; Wu, W.; Yu, Z.; Shen, Y. Nonlinear optical spectroscopy of photonic metamaterials. *Phys. Rev. B: Condens. Matter Mater. Phys.* **2008**, *78*, 113102.
(37) Ciracì, C.; Poutrina, E.; Scalora, M.; Smith, D. R. Origin of second-harmonic generation enhancement in optical split-ring resonators. *Phys. Rev. B: Condens. Matter Mater. Phys.* **2012**, *85*, 201403.
(38) Poutrina, E.; Huang, D.; Urzhumov, Y.; Smith, D. R. Nonlinear oscillator metamaterial model: numerical and experimental verification. *Opt. Express* **2011**, *19*, 8312−8319.
(39) Rose, A.; Huang, D.; Smith, D. R. Nonlinear Interference and Unidirectional Wave Mixing in Metamaterials. *Phys. Rev. Lett.* **2013**, *110*, 063901.
(40) Dolling, G.; Enkrich, C.; Wegener, M.; Zhou, J. F.; Soukoulis, C. M.; Linden, S. Cut-wire pairs and plate pairs as magnetic atoms for optical metamaterials. *Opt. Lett.* **2005**, *30*, 3198−3200.
(41) Shalaev, V. M.; Cai, W.; Chettiar, U. K.; Yuan, H.-K.; Sarychev, A. K.; Drachev, V. P.; Kildishev, A. V. Negative index of refraction in optical metamaterials. *Opt. Lett.* **2005**, *30*, 3356−3358.
(42) Shcherbakov, A. A.; Tishchenko, A. V. New fast and memory-sparing method for rigorous electromagnetic analysis of 2D periodic dielectric structures. *J. Quant. Spectrosc. Radiat. Transfer* **2012**, *113*, 158−171.
(43) Heinz, T. F. In *Nonlinear Surface Electromagnetic Phenomena*; Ponath, H. E., Stegeman, G. I., Eds.; Elsevier: Amsterdam, 1991; Chapter 5, pp 353−416.
(44) Krause, D.; Teplin, C. W.; Rogers, C. T. Optical surface second harmonic measurements of isotropic thin-film metals: Gold, silver, copper, aluminum, and tantalum. *J. Appl. Phys.* **2004**, *96*, 3626−3634.
(45) Wang, F. X.; Rodriguez, F. J.; Albers, W. M.; Ahorinta, R.; Sipe, J. E.; Kauranen, M. Surface and bulk contributions to the second-order nonlinear optical response of a gold film. *Phys. Rev. B: Condens. Matter Mater. Phys.* **2009**, *80*, 233402.
(46) Weismann, M.; Gallagher, D. F. G.; Panoiu, N. C. Nonlinear generalized source method for modeling second-harmonic generation in diffraction gratings. *J. Opt. Soc. Am. B* **2015**, *32*, 523−533.
(47) Dadap, J. I.; Shan, J.; Heinz, T. F. Theory of optical second-harmonic generation from a sphere of centrosymmetric material: small-particle limit. *J. Opt. Soc. Am. B* **2004**, *21*, 1328.
(48) Cao, L.; Panoiu, N. C.; Bhat, R. D. R.; Osgood, R. M. Surface second-harmonic generation from scattering of surface plasmon polaritons from radially symmetric nanostructures. *Phys. Rev. B: Condens. Matter Mater. Phys.* **2009**, *79*, 235416.

DOI: 10.1021/acsphotonics.5b00215
ACS Photonics 2015, 2, 1007−1012